

**Strongly nonlinear long gravity waves in uniform shear flows**

Wooyoung Choi

*Department of Naval Architecture and Marine Engineering, University of Michigan, Ann Arbor, Michigan 48109, USA*

(Received 14 January 2003; published 12 August 2003)

Long surface gravity waves of finite amplitude in uniform shear flows are considered by using an asymptotic model derived under the assumption that the aspect ratio between wavelength and water depth is small. Since its derivation requires no assumption on wave amplitude, the model can be used to describe arbitrary amplitude waves. It is shown that the simple model captures the interesting features of strongly nonlinear solitary waves observed in previous numerical solutions. When compared with the case of zero vorticity, the solitary wave in uniform shear flows is wider when propagating upstream (opposite to the direction of surface drift), while it is narrower when propagating downstream. For the upstream-propagating solitary wave, a stationary recirculating eddy appears at the bottom when wave amplitude exceeds the critical value. For the case of downstream propagation, no eddy forms at the bottom but the solitary wave becomes more peaked, yielding a cusp at the critical wave amplitude, beyond which the solitary wave has a round wave profile. Although the appearance of the derivative singularity is inconsistent with the long-wave assumption in the model, round wave profiles away from the singularity are qualitatively similar to numerical solutions and observation.

DOI: 10.1103/PhysRevE.68.026305

PACS number(s): 47.32.-y, 47.35.+i, 47.15.Ki

**I. INTRODUCTION**

When gravity waves propagate on the surface of shear flows, it is no longer appropriate to adopt the assumption of irrotational flows under which most theories for surface waves have been developed. See, for example, Mei [1] for a review of irrotational water wave theories and Choi [2] for recent advances. Linear long gravity waves in shear flows were first considered by Burns [3], who examined the range of long-wave speed for general velocity profiles. For linear gravity waves of arbitrary wavelength in water of finite depth, Yih [4] investigated the linear stability of shear flows in detail.

After Benjamin [5] developed a weakly nonlinear theory for steady solitary waves, Freeman and Johnson [6] derived the Korteweg–de Vries equation to describe the time evolution of weakly nonlinear waves in shear flows of arbitrary vorticity distribution, but little progress has been made beyond the weakly nonlinear regime. When a strong shear current is present in shallow water, it has been shown that the effect of strong nonlinearity on the propagation of surface gravity waves needs to be taken into consideration [7].

To isolate the effect of background vorticity and to avoid mathematical complexity, a simple case of constant vorticity has been often considered by assuming that the detailed vorticity distribution is unimportant for long waves. Even for this simple uniform shear for which all perturbations are irrotational, only numerical approaches using the boundary integral method have been adopted to find finite amplitude solitary wave solutions [7–9]. Numerical solutions for steady waves are valuable but it is rather difficult to study their time evolution with the full Euler equations. Therefore a simple model capturing the salient features of strongly nonlinear waves will be very useful.

Here we derive an asymptotic model for long surface gravity waves of large amplitude in shallow water of constant vorticity and analytically study strongly nonlinear solitary wave solutions. The derivation of the model based on a

systematic expansion method is presented in Sec. III. The ratio between water depth and characteristic wavelength is assumed to be small but no assumption on wave amplitude is imposed. Similar asymptotic expansion methods have been successfully applied to interfacial gravity waves between two fluids [10–12]. Solitary wave solutions of the model are compared with weakly and fully nonlinear solutions in Sec. IV.

**II. BASIC EQUATIONS**

For an inviscid and incompressible fluid of density  $\rho$ , the two-dimensional velocity components ( $U, V$ ) in Cartesian coordinates and the pressure  $P$  satisfy the Euler equations and the continuity equation given by

$$U_t + UU_x + VU_y = -P_x/\rho, \quad (1)$$

$$V_t + UV_x + VV_y = -P_y/\rho - g, \quad (2)$$

$$U_x + V_y = 0, \quad (3)$$

where  $g$  is the gravitational acceleration. Since the equation for vorticity  $\omega (= V_x - U_y)$  is given, from Eqs. (1)–(3), by  $d\omega/dt = 0$ , any two-dimensional perturbations to flow with constant vorticity are irrotational. The boundary conditions at the free surface and the bottom are given by

$$\zeta_t + U\zeta_x = V, \quad P = 0 \quad \text{at } y = h + \zeta(x, t), \quad (4)$$

$$V = 0 \quad \text{at } y = 0, \quad (5)$$

where  $\zeta(x, t)$  is the surface elevation and  $h$  is the water depth.

For the case of constant negative vorticity  $\omega = -\Omega$ , as shown in Fig. 1, the dispersion relation between linear wave speed  $c_l$  and wave number  $k$  is given [7] by

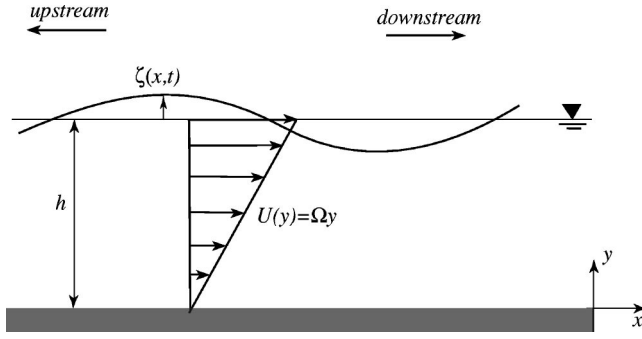


FIG. 1. Uniform shear flow.

$$\frac{c_l^\pm}{\sqrt{gh}} = F \left( 1 - \frac{\tanh(kh)}{2kh} \right) \pm \sqrt{\frac{\tanh(kh)}{kh} \left( 1 + F^2 \frac{\tanh(kh)}{4kh} \right)}, \quad (6)$$

where the Froude number  $F$  is defined by

$$F = \frac{\Omega h}{\sqrt{gh}}. \quad (7)$$

As  $kh \rightarrow 0$ ,  $c_l$  is reduced to the linear long-wave speed,  $c_0$ , given by

$$\frac{c_0^\pm}{\sqrt{gh}} = \frac{F}{2} \pm \sqrt{1 + \frac{F^2}{4}}. \quad (8)$$

### III. MODEL FOR STRONGLY NONLINEAR LONG WAVES

To derive the model, we first nondimensionalize physical variables as

$$x = Lx^*, \quad y = hy^*, \quad t = (L/\sqrt{gh})t^*, \quad (9)$$

$$P = (\rho gh)P^*, \quad \zeta = h\zeta^*, \quad U = \sqrt{gh}U^*, \quad V = \epsilon\sqrt{gh}V^*, \quad (10)$$

where  $L$  is a typical horizontal length scale and  $\epsilon = h/L$  is assumed to be small for long waves. When we substitute Eqs. (9) and (10) into the horizontal momentum equation (1) and the continuity equation (3), we have, after taking the depth mean of the equations and dropping all the asterisks [11],

$$\eta_t + (\eta \bar{U})_x = 0, \quad \eta = 1 + \zeta(x, t), \quad (11)$$

$$(\eta \bar{U})_t + (\eta \overline{UU})_x = -\eta \bar{P}_x, \quad (12)$$

where  $\bar{f}$  is the depth mean quantity defined by

$$\bar{f}(x, t) = \frac{1}{\eta} \int_0^{1+\zeta} f(x, y, t) dy. \quad (13)$$

The vertical momentum equation (2) can be written as

$$P_y = -1 - \epsilon^2 [V_t + UV_x + VV_y], \quad (14)$$

and the vorticity  $\omega$  is given by

$$\omega = -U_y + \epsilon^2 V_x. \quad (15)$$

For uniform shear flow, the velocity field can be decomposed into

$$(U, V) = (U_0 + u, v), \quad U_0(y) = Fy, \quad (16)$$

where  $U_0(y)$  is the rotational basic flow and  $(u, v)$  are the irrotational perturbation velocity components.

From Eqs. (14) and (15), we assume that all physical variables for irrotational flows can be expanded as

$$f(x, y, t) = f_0 + \epsilon^2 f_1 + O(\epsilon^4), \quad f = (u, v, P). \quad (17)$$

Substituting Eqs. (16) and (17) into Eqs. (14) and (15) with  $\omega = -F$ , we have the leading-order equation as

$$u_{0y} = 0, \quad v_{0y} = -u_{0x}, \quad P_{0y} = -1, \quad (18)$$

where the continuity equation  $u_x + v_y = 0$  has been used. Then the first-order solutions can be found as

$$u_0 = u_0(x, t), \quad v_0 = -u_{0x}y, \quad P_0 = -(y - \eta), \quad (19)$$

where the boundary conditions,  $v = 0$  at  $y = 0$  and  $P = 0$  at  $y = \eta$ , have been imposed.

Similarly the second-order solutions can be found, at  $O(\epsilon^2)$ , as

$$u_1(x, y, t) = -\frac{1}{2} u_{0xx} y^2 + f_1(x, t),$$

$$v_1(x, y, t) = \frac{1}{6} u_{0xxx} y^3 + f_{1x} y^2, \quad (20)$$

and, from Eq. (14), the second-order pressure  $P_1$  is given by

$$P_1 = \frac{1}{2} G(x, t)(y^2 - \eta^2) + \frac{F}{3} u_{0xx}(y^3 - \eta^3), \quad (21)$$

where

$$G(x, t) = u_{0xt} + u_0 u_{0xx} - u_{0x}^2. \quad (22)$$

From Eqs. (19) and (21), the right-hand side of Eq. (12) is obtained as

$$\bar{P}_x = \zeta_x - \frac{1}{\eta} \left( \frac{1}{3} \eta^3 G + \frac{F}{4} \eta^4 \bar{u}_{xx} \right) + O(\epsilon^4). \quad (23)$$

Also, from Eq. (16),  $\eta \bar{U}$  and  $\eta \overline{UU}$  in the left-hand sides of Eqs. (11) and (12) can be written as

$$\eta \bar{U} = \eta \left( \frac{F}{2} \eta + \bar{u} \right), \quad \eta \overline{UU} = \eta \left( \frac{F^2}{3} \eta^3 + 2 \overline{U_0 u} + \overline{uu} \right), \quad (24)$$

and, from Eqs. (19) and (20), we have found that

$$2\eta\overline{U_0u} = F\left(\eta^2\bar{u} - \frac{1}{12}\eta^4\bar{u}_{xx}\right) + O(\epsilon^4),$$

$$\overline{\eta uu} = \eta\bar{u}\bar{u} + O(\epsilon^4). \tag{25}$$

By substituting Eqs. (23) and (25) into Eqs. (11) and (12), we finally obtain, after some manipulation, the following evolution equations for  $\bar{u}$  and  $\eta$ :

$$\eta_t + F\eta\eta_x + (\eta\bar{u})_x = 0, \tag{26}$$

$$\bar{u}_t + \bar{u}\bar{u}_x + \zeta_x = \frac{1}{\eta}\left[\frac{\eta^3}{3}(\bar{u}_{xt} + \bar{u}\bar{u}_{xx} - \bar{u}_x^2 + F\eta\bar{u}_{xx})\right]_x. \tag{27}$$

Since we have imposed no assumption on wave amplitude, the system of Eqs. (26) and (27) can be regarded as a model for strongly nonlinear long waves. The first equation implying the mass conservation is exact and the second equation from the horizontal momentum equation has an error of  $O(\epsilon^4)$ . The horizontal momentum equation (27) can be rewritten, in a conserved form, as

$$\left(\bar{u} + \frac{1}{6}\eta^2\bar{u}_{xx}\right)_t + \left(\frac{1}{2}\bar{u}^2 + \eta\right)_x = \left[\frac{\eta^2}{2}(\bar{u}_{xt} + \frac{2}{3}\bar{u}\bar{u}_{xx} - \bar{u}_x^2 + \frac{2}{3}F\eta\bar{u}_{xx})\right]_x \tag{28}$$

or, after multiplying by  $\eta$ , as

$$\left(\eta\bar{u} + \frac{F}{2}\eta^2\right)_t + \left(\eta\bar{u}^2 + \frac{1}{2}\eta^2 + F\eta^2\bar{u} + \frac{F^2}{3}\eta^3\right)_x = \left[\frac{\eta^3}{3}(\bar{u}_{xt} + \bar{u}\bar{u}_{xx} - \bar{u}_x^2 + F\eta\bar{u}_{xx})\right]_x. \tag{29}$$

These two different forms of equations imply conservation of vorticity and momentum, respectively.

When no shear is present ( $F=0$ ), Eqs. (26) and (27) can be reduced to the set of equations, first derived by Green and Naghdi [13] using the so-called director-sheet method, whose solitary wave solution is given by

$$\zeta = a \operatorname{sech}^2[k(x-ct)], \quad k^2 = \frac{3a}{4(1+a)}, \quad c^2 = 1+a. \tag{30}$$

It is well known that the highest irrotational solitary wave has a  $120^\circ$  angle at the crest, where the long-wave approximation ceases to be valid. Therefore the irrotational model with  $F=0$  becomes invalid as wave amplitude approaches the maximum value.

**Weakly nonlinear waves**

For weakly nonlinear waves of  $a/h = O(\epsilon^2)$  where  $a$  is typical wave amplitude, Eqs. (26) and (27) can be reduced to the Boussinesq equations if we substitute  $\eta=1$  and neglect the quadratic nonlinear terms in the right-hand side of Eq. (27). The kinematic equation is the same as Eq. (26), while the dynamic equation becomes

$$\bar{u}_t + \bar{u}\bar{u}_x + \zeta_x = \frac{1}{3}(\bar{u}_{xxt} + F\bar{u}_{xxx}). \tag{31}$$

For unidirectional waves, we can reduce the system of equations given by Eqs. (26) and (31) to the Korteweg–de Vries (KdV) equation [5,6]:

$$\zeta + c_0\zeta_x + c_1\zeta\zeta_x + c_2\zeta_{xxx} = 0, \tag{32}$$

where  $c_0$  is defined in Eq. (8) and  $c_1$  and  $c_2$  are given by

$$c_1 = \frac{(c_0 - F)^3 + 2(c_0 - F) + F}{1 + (c_0 - F)^2}, \quad c_2 = \frac{(c_0 - F)^3}{3[1 + (c_0 - F)^2]}. \tag{33}$$

The well-known solitary wave solution of Eq. (32) is given by

$$\zeta = a \operatorname{sech}^2[k(x-ct)], \quad k^2 = \frac{ac_1}{12c_2}, \quad c = c_0 + \frac{ac_1}{3}. \tag{34}$$

**IV. SOLITARY WAVES**

For traveling waves, we assume

$$\zeta = \zeta(X), \quad \bar{u} = \bar{u}(X), \quad X = x - ct. \tag{35}$$

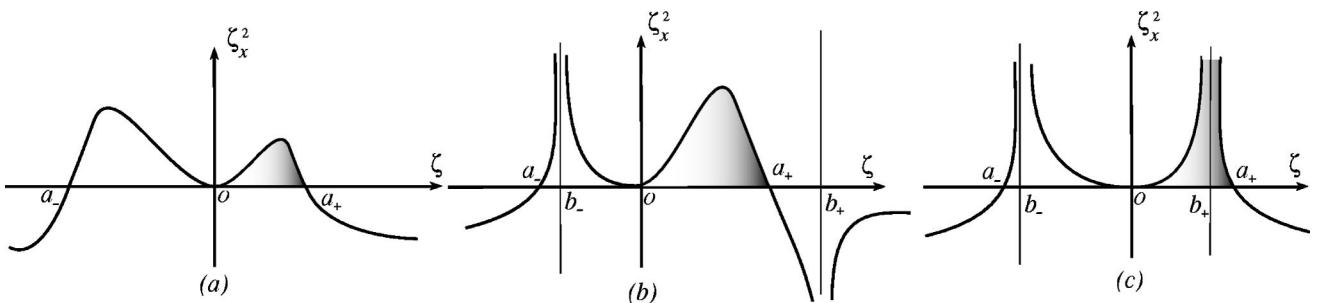


FIG. 2. The right-hand side of Eq. (37) shows that solitary wave solutions exist only in shaded areas. (a) Upstream-propagating solitary waves of  $c=c^-$ , (b) subcritical solitary waves propagating downstream ( $c=c^+$ ,  $a_+ < b_+$ ), (c) supercritical solitary waves ( $c=c^+$ ,  $a_+ > b_+$ ).

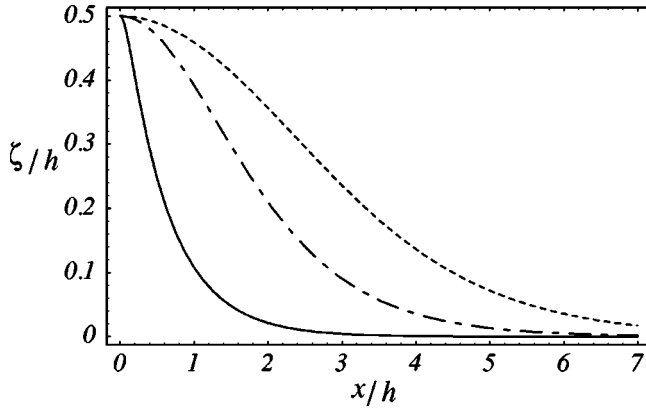


FIG. 3. Solitary wave profiles of wave amplitude  $a=0.5$ : downstream-propagating waves (—) with  $F=1$ ; upstream-propagating waves (- - -) with  $F=1$ ; pure gravity waves (- · - ·) with  $F=0$ .

After substituting Eq. (35) into Eq. (26) and integrating once, we obtain the following expression for  $\bar{u}$  in terms of  $\eta$

$$\bar{u} = c \left( 1 - \frac{1}{\eta} \right) + \frac{F}{2} \left( \frac{1}{\eta} - \eta \right), \quad (36)$$

where we have imposed the zero boundary conditions for  $\zeta$  and  $\bar{u}$  at both infinities. After integrating once the two different forms of the horizontal momentum equations given by Eqs. (28) and (29), and subtracting each other, we have the following first-order ordinary differential equation for  $\zeta$ :

$$\zeta_x^2 = \frac{\zeta^2(a_+ - \zeta)(\zeta - a_-)}{(\zeta - b_+)^2(\zeta - b_-)^2} \equiv \frac{\zeta^2 N[\zeta]}{D[\zeta]^2}, \quad (37)$$

where we have used Eq. (36) and imposed the zero boundary conditions at both infinities for  $\zeta$  and  $\zeta_x$  to find solitary wave solutions. In Eq. (37),  $a_{\pm}$  are two roots of  $N[\zeta]=0$  given by

$$N[\zeta] = -\zeta^2 - \left( 4 + \frac{12}{F^2} \right) \zeta + \left( \frac{12}{F^2} \right) (c^2 - Fc - 1) = 0, \quad (38)$$

and  $b_{\pm}$  are two roots of  $D[\zeta]=0$  given by

$$D[\zeta] = \zeta^2 + 2\zeta + 2 \left( 1 - \frac{c}{F} \right) = 0. \quad (39)$$

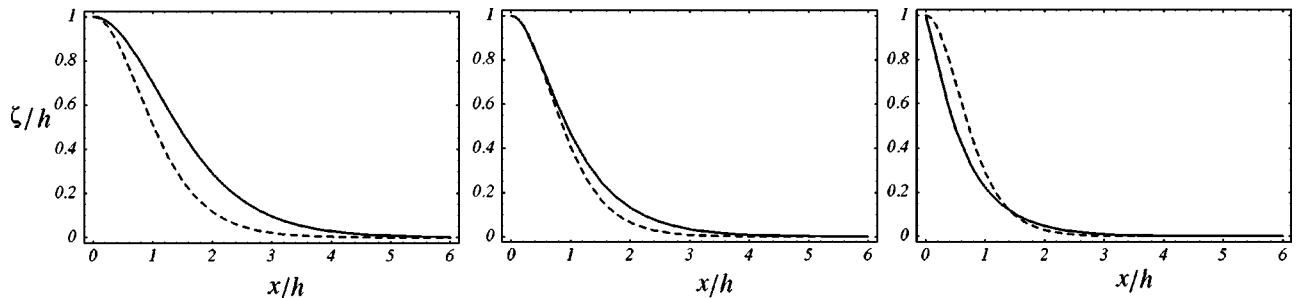


FIG. 5. Subcritical case: comparison of strongly nonlinear solitary waves of  $a=1$  (—) propagating downstream, governed by Eq. (37), with weakly nonlinear waves (- - -) governed by Eq. (32) for three different (subcritical) Froude numbers ( $F=0, 0.3, 0.6$ ).

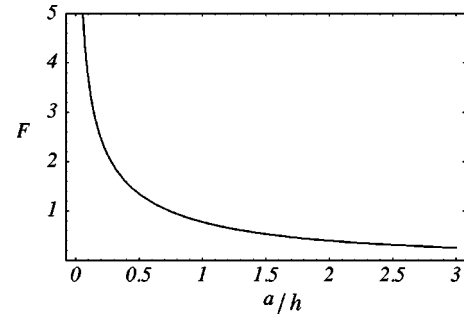


FIG. 4. The critical condition between the Froude number and wave amplitude, given by Eq. (41).

For solutions of Eq. (37) to be bounded and physical ( $\zeta > -1$ ), a solitary wave has to be always positive with wave amplitude  $a \equiv a_+$ . Note that  $a_-$  is always less than  $-1$ , which is unphysical. By setting  $\zeta_x=0$  (equivalently,  $N[\zeta]=0$ ) at  $\zeta=a$ , the wave speed  $c$  can be found as

$$c^{\pm}(a) = \frac{F}{2} \pm \sqrt{1 + a + \frac{F^2}{12}(a^2 + 4a + 3)}, \quad (40)$$

which can be reduced to the linear long-wave speed  $c_0^{\pm}$  as  $a \rightarrow 0$ . The left- and right-going waves have wave speed of  $c^- < c_0^- < 0$  and  $c^+ > c_0^+ > 0$ , respectively.

As illustrated in Fig. 2, there are three cases of interest depending on the behavior of the denominator of Eq. (37). For upstream-propagating waves ( $c=c^-$ ), the denominator of Eq. (37) never vanishes and solitary wave solutions always exist for all wave amplitudes [see Fig. 2(a)]. For downstream-propagating waves ( $c=c^+$ ),  $c > (F/2)$  and the denominator of Eq. (37) may vanish at  $\zeta=b_{\pm}$ . In particular,  $b_+ > 0$  deserves attention since  $b_+$  can lie in between the interval  $0 < b_+ < a$ , which is the physical range of  $\zeta$ . When the wave amplitude is small,  $b_+$  is greater than  $a$  and no singularity appears inside the physical range of  $\zeta$  (Fig. 2b). As the wave amplitude increases,  $a$  approaches  $b_+$  and both numerator and denominator vanish at the critical wave amplitude ( $a=b_+$ ). This critical condition between wave amplitude and the Froude number can be written, from Eqs. (38) and (39), as

$$F^2 = \frac{12}{3a^3 + 9a^2 + 8a}. \quad (41)$$

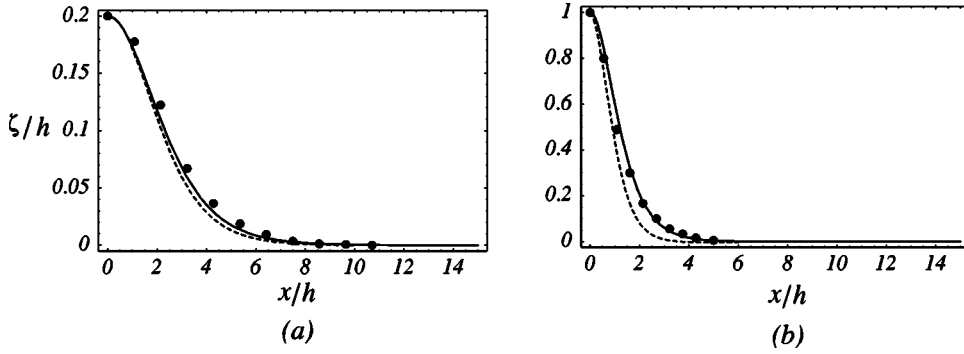


FIG. 6. Solitary wave solutions (—) of Eq. (37) compared with weakly nonlinear solitary waves (- - -) governed by Eq. (32), and numerical solutions (●) by Vanden-Broeck [8]. (a)  $a = 0.2$ ,  $F = 0.114$ ; (b)  $a = 1$ ,  $F = 0.148$ .

Beyond the critical wave amplitude, the slope becomes infinite ( $\zeta_X = \infty$ ) at a point where  $\zeta = b_+$  [Fig. 2(c)].

Solitary wave solutions can be found implicitly, by integrating Eq. (37), as

$$\text{case (a): } X = -H[\zeta; c^-] + H[a_+; c^-],$$

$$\text{case (b): } X = H[\zeta; c^+] - H[a_+; c^+],$$

$$\text{case (c): } X = -H[\zeta; c^+] + H[a_+; c^+] \quad \text{for } b_+ \leq \zeta \leq a_+$$

$$X = H[\zeta; c^+] - H[b_+; c^+] + X_0 \quad \text{for } 0 \leq \zeta \leq b_+,$$

where

$$H[\zeta; c] = \int^\zeta \frac{D[\zeta]}{\zeta \sqrt{N[\zeta]}} d\zeta = -\sqrt{N[\zeta]} - \left(\frac{6}{F^2}\right) \sin^{-1}\left(\frac{2\zeta + \beta}{2a_+ + \beta}\right) + \frac{2(1 - c/F)}{\sqrt{a_+^2 + \beta a_+}} (\ln \zeta - \ln[2(a_+^2 + \beta a_+) - \beta \zeta] + 2\sqrt{(a_+^2 + \beta a_+)N[\zeta]}),$$

$$X_0 = H[a_+, c^+] - H[b_+, c^+], \text{ and } \beta = 4 + 12/F^2.$$

Before we present wave profiles for different regimes, we first compare in Fig. 3 irrotational ( $F=0$ ) and rotational ( $F=1$ ) solitary waves of  $a=0.5$  propagating upstream and downstream. Since waves are symmetric, we only show a half of the wave profile. As pointed out by Benjamin [5] based on his weakly nonlinear theory, the vorticity typically lengthens the solitary wave propagating opposite to the direction of surface drift, while it shortens the wave propagating in the same direction of surface drift.

### A. Waves propagating downstream

For fixed  $a$  (or  $F$ ), as shown in Fig. 4, the condition given by Eq. (41) determines the critical Froude number  $F_c$  (or the critical wave amplitude  $a_c$ ). For example, when  $a=1$ , the critical Froude number is  $F_c = \sqrt{15/5} \approx 0.775$ . For the subcritical case ( $F < F_c$ ), as the Froude number approaches to the critical value, Fig. 5 shows that solitary waves become more peaked. When compared with weakly nonlinear waves, we can see that strongly nonlinear waves become narrower as the Froude number  $F$  increases. In Fig. 6, solitary wave solutions of Eq. (37) for the subcritical case are compared with exact numerical solutions by Vanden-Broeck [8], and we note that the strongly nonlinear model shows better agreement than the weakly nonlinear KdV model as wave amplitude increases.

As the Froude number further increases and reaches the critical value given by Eq. (41), solitary wave is finite but has a cusp at the peak with  $\zeta_X(0) \rightarrow \infty$ . Beyond the criticality, although the derivative singularity appears at  $X = X_0$  where  $\zeta(X_0) = b_+$  with  $0 < b_+ < a$ , strongly nonlinear solitary waves become round. Figure 7 shows wave profiles for three different supercritical Froude numbers ( $F=1, 2, 4$ ), and the weakly nonlinear theory never describes this type of solitary wave. Wave profiles of higher amplitude  $a = 10, 20$ , and  $40$  for  $F=1$  are shown in Fig. 8

From Eq. (37), the behavior of  $\zeta_X$  near  $X = X_0$  is approximated by  $\zeta_X \sim -1/(\zeta - b_+)$  and its solution can be found as  $\zeta - b_+ \sim \pm |X - X_0|^{1/2}$ , where the positive (negative) sign is taken for  $X < X_0$  ( $X > X_0$ ). Therefore we can see that the supercritical solitary wave solution has the square-root singularity in the derivative.

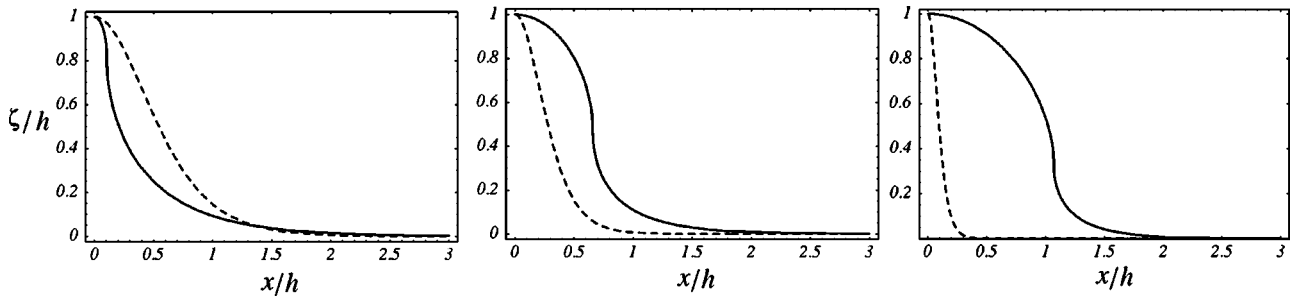


FIG. 7. Supercritical case: comparison of strongly nonlinear solitary waves of  $a=1$  (—) propagating downstream, governed by Eq. (37), with weakly nonlinear waves (- - -) governed by Eq. (32) for three different (supercritical) Froude numbers ( $F=1, 2, 4$ ).

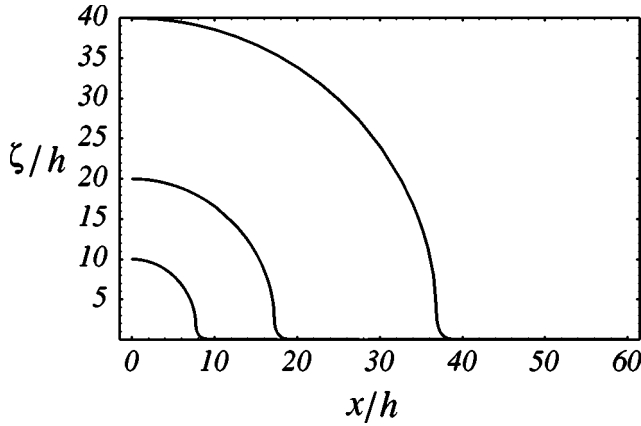


FIG. 8. Strongly nonlinear solitary waves of  $a=10, 20,$  and  $40$  with  $F=1$  propagating downstream.

**B. Waves propagating upstream**

For upstream-propagating waves ( $c=c^-$ ), the denominator never vanishes for real  $\zeta$  and  $b_{\pm}$  is purely imaginary. Therefore smooth solitary waves exist for any wave amplitude and Froude number, as shown in Fig. 9. When compared with the KdV theory, upstream propagating solitary waves of large amplitude are always wider than weakly nonlinear waves.

As the leading-order approximation, the total stream function  $\Psi$  can be written, in a frame moving with wave speed  $c$ , as

$$\Psi(X,y) = \frac{F}{2}y^2 - cy + \bar{u}(X)y, \quad (42)$$

which, at the bottom and the free surface, becomes  $\Psi(X,0) = 0$  and  $\Psi(X,\eta) = -c + (F/2)$ , respectively. At  $X=0$ ,  $\Psi$  in Eq. (42) can be rewritten, from Eq. (36), as

$$\Psi(0,y) = \frac{F}{2}y(y-y_0), \quad (43)$$

where  $y_0$  is given by

$$y_0 = a + 1 + \frac{(2c/F) - 1}{a + 1}. \quad (44)$$

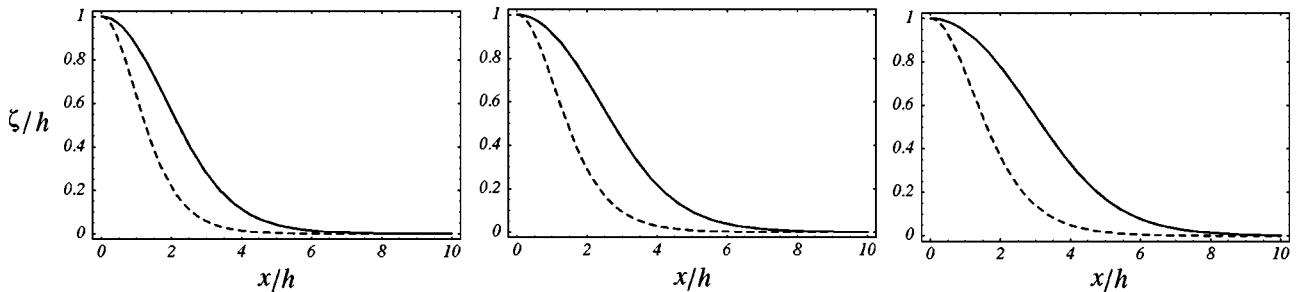


FIG. 9. Comparison of strongly nonlinear solitary waves of  $a=1$  (—) propagating upstream, governed by Eq. (37), with weakly nonlinear waves (- - -) governed by Eq. (32) for different Froude numbers ( $F=0.5,1,2$ ).

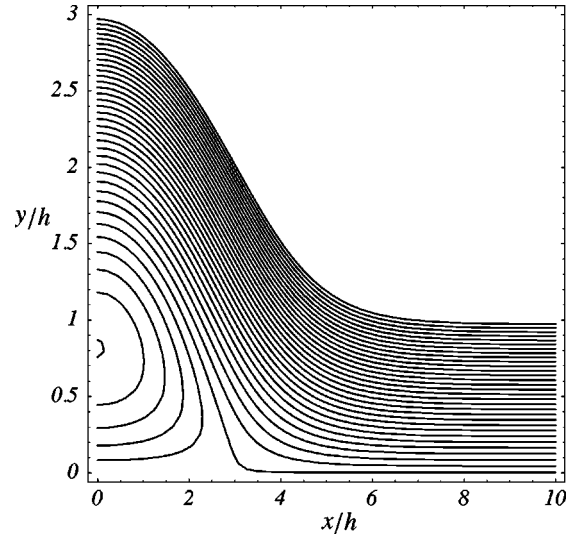


FIG. 10. Streamlines for a upstream-propagating solitary wave with  $F=1$  and  $a=2$ .

From Eq. (43), when  $c < (F/2)$ , we can see that the sign of stream function  $\Psi$  can change from negative to positive in between the bottom and the free surface ( $0 < y < 1+a$ ), when  $y_0$  is positive. This implies that there is a chance for a recirculating eddy of amplitude  $y_0$  to appear at the bottom. This happens only to upstream-propagating waves when the wave amplitude is large enough. For  $y_0$  to be positive and less than  $a+1$ , we have, from Eq. (44), the following condition

$$\frac{F}{2}[1 - (a+1)^2] < c < \frac{F}{2}. \quad (45)$$

It is interesting to note that, from the condition given by Eq. (45), the minimum wave amplitude for a stationary eddy to appear is exactly the same as that for the occurrence of singularity in  $\zeta_x$  given by Eq. (41). For example, the minimum wave amplitude for  $F=1$  is  $a \approx 0.738$  and the size of the eddy grows as wave amplitude increases. Figure 10 shows the streamlines for the Froude number  $F=1$  and wave amplitude  $a=2$ , and a well-defined eddy is observed.

**V. DISCUSSION**

We have derived a set of evolution equations for strongly nonlinear long waves in uniform shear flows and found large

amplitude solitary wave solutions propagating both upstream and downstream. A solitary wave propagating opposite to the direction of surface drift (upstream) can induce a steady recirculating eddy at the bottom when wave amplitude exceeds the critical value. For waves propagating in the same direction as the surface drift, smooth solitary waves cease to exist at the critical wave amplitude, beyond which new round solitary wave solutions with infinite wave slopes symmetrically disposed on both sides of the wave are found.

The appearance of the derivative singularity for large amplitude waves in shear flows is somewhat puzzling since it is inconsistent with the original long-wave assumption in the model. This singularity disappears at the irrotational limit ( $F=0$ ) and therefore is associated with pure rotational wave modes in a thin layer of constant vorticity. In other words, solitary wave solutions of the same problem without gravity ( $g=0$ ) will also have the derivative singularity. Previous numerical solutions [7,8] in fact show that rotational solitary wave has a corner of  $120^\circ$  at the critical (not necessarily

maximum) wave amplitude, beyond which waves become round and multivalued in the limit of zero gravity. Any long-wave model cannot describe a multivalued wave profile and a solution with infinite slope can be considered as an approximation to such a wave profile. Round and wider solitary wave solutions away from the singularity are qualitatively similar to what have been observed in the surf zone [7] and earlier numerical solutions of the full Euler equations [8]. More careful comparison with numerical solutions is necessary to validate our solutions for very large amplitude round waves.

Here we only consider traveling wave solutions but, by using the model, one can study the evolution of large rotational solitary waves, including their stability and interaction. Also the effect of bottom topography can be easily included in the model and it would be interesting to examine whether the rotational model better predicts the dynamics of shallow water waves in the surf zone, where the horizontal vorticity is easily generated by wave breaking.

- 
- [1] C.C. Mei, *The Applied Dynamics of Ocean Surface Waves* (World Scientific, River Edge, NJ, 1989).  
 [2] W. Choi, *J. Fluid Mech.* **295**, 381 (1995).  
 [3] J.C. Burns, *Proc. Cambridge Philos. Soc.* **49**, 695 (1953).  
 [4] C.S. Yih, *J. Fluid Mech.* **51**, 209 (1972).  
 [5] T.B. Benjamin, *J. Fluid Mech.* **12**, 97 (1962).  
 [6] N.C. Freeman and R.S. Johnson, *J. Fluid Mech.* **42**, 401 (1970).  
 [7] A.F. Teles da Silva and D.H. Peregrine, *J. Fluid Mech.* **195**, 281 (1988).  
 [8] J.-M. Vanden-Broeck, *J. Fluid Mech.* **274**, 339 (1994).  
 [9] R.A. Dalrymple, *J. Geophys. Res.* **79**, 4498 (1974).  
 [10] W. Choi and R. Camassa, *Phys. Rev. Lett.* **77**, 1759 (1996).  
 [11] W. Choi and R. Camassa, *J. Fluid Mech.* **396**, 1 (1999).  
 [12] T. Jo and W. Choi, *Stud. Appl. Math.* **109**, 205 (2002).  
 [13] A.E. Green and P.M. Naghdi, *J. Fluid Mech.* **78**, 237 (1976).